行政院國家科學委員會專題研究計畫 期中進度報告

加速旋轉與震動控制的垂直布氏法單晶生長之研究與應用 (2/3)

期中進度報告(精簡版)

計 畫 類 別 ：個別型
計 畫 編 號 ：NSC 95-2221-E-002-306-
執 行 期 間 ：95 年 08 月 01 日至 96 年 07 月 31 日
執 行 單 位 ：國立臺灣大學化學工程學系暨研究所

計 畫 主 持 人 ：藍崇文

處 理 方 式 ：本計畫可公開查詢

中 華 民 國 96 年 10 月 30 日

行政院國家科學委員會補助專題研究計畫 □ 成 果 報 告 V 期中進度報告

加速旋轉與震動控制的垂直布氏法單晶生長之研究與應用(2/3)

計畫類別：v 個別型計畫　　□ 整合型計畫

計畫編號：NSC 95-2221-E-002-306

執行期間：2006/08/01～2007/07/31

計畫主持人： 藍崇文

共同主持人： 無

計畫參與人員： 劉有晟、王亮程、陳志彬

成果報告類型(依經費核定清單規定繳交)：V 精簡報告　□完整報告

本成果報告包括以下應繳交之附件：

□赴國外出差或研習心得報告一份

□赴大陸地區出差或研習心得報告一份

□出席國際學術會議心得報告及發表之論文各一份

□國際合作研究計畫國外研究報告書一份

處理方式：除產學合作研究計畫、提升產業技術及人才培育研究計畫、列管計畫及下列情形者外，得立即公開查詢

□涉及專利或其他智慧財產權，□一年□二年後可公開查詢

執行單位：國立台灣大學化學工程學所

中　華　民　國　96　年　10　月　30　日

Segregation control by accelerated crucible rotation for vertical Bridgman crystal growth of Ga-doped Ge: ACRT versus angular vibration

L.C. Wang[a], Y.C. Liu[a], B. Roux[b], T. P. Lyubimova[c], C.W. Lan[a*]

a Department of Chemical Engineering, National Taiwan University,
Taipei, Taiwan, 10617, ROC

b Laboratoire Modélisation et simulation numérique en mécanique, L3M / FRE 2405 MSNM:
CNRS-Universités d'Aix-Marseille, France

c Institute of Continuous Media Mechanics UB RAS, Perm, Russia

Keywords: A1: Segregation; Convection; Accelerated crucible rotation Technology; B2: Bridgman method

*Corresponding author: cwlan@ntu.edu.tw; Tel (Fax): 886-2-2363-3917

中文摘要

在本研究成果報告書當中，我們將加速旋轉坩堝對晶體生長之偏析行為的影響應用到垂直布氏法鍺摻鎵晶體的實際生長實驗，在兩種不同拉速下的晶體生長結果中，我們再次證明了加速旋轉坩堝的 ACRT 會輕微地影響整體熔湯的混合，而 AVT 能夠輕易地在不影響熔湯混合的情況下達到改善徑向偏析的目的，此兩種加速旋轉坩堝法皆能改善徑向的偏析情況，而 AVT 能夠更有效地進一步控制晶體成長的行為。

Abstract

The control of segregation by accelerated crucible rotation is investigated by the experiment of vertical Bridgman crystal growth of Ga-doped Ge. It was shown that the concentration distribution under two different pulling rates. It is clear that ACRT generates the global mixing slightly. On the other hand, angular vibration technique (AVT) can reverse the radial segregation easily without enhancing the global mixing. Although both techniques can reduce radial segregation, AVT is more effective for growth control.

1. Introduction

The control of convection and segregation is important in vertical Bridgman (VB) crystal growth crystal growth. Because of a lack of control over stirring conditions, the use of external forces is often adopted. Scheel and Schulz-DuBois proposed an accelerated crucible rotation technique (ACRT) to control the melt mixing [1]. By controlling the acceleration cycle, it is possible to control the melt mixing at either an enhanced mixing [2-4] or diffusion-limited mode [5]. The effects of ACRT also depend on the ratio of the melt depth to the size of Ekman cells, on the buoyant convection, and on the vortices that sometimes form due to the Taylor-Görtler instability near the ampoule wall [6-8] Therefore, ACRT is believed to be useful

for vertical Bridgman crystal growth.

Nevertheless, it is still controversial whether or not ACRT is the best method of growth control, because the issues of growth striations, radial, axial segregations need to be judged carefully. Therefore, an alternative approach to applying ACRT is to use a cycle time that is much shorter than the Ekman time. This method is known as the angular vibration technique (AVT) [9]. In this technique, the ampoule is vibrated at high frequency (typically greater than 5Hz). In a recent experimental and numerical study of a transparent system, effects of axial and radial segregation by this technique were investigated [9-12].

In this paper, we present the experimental results from a Bridgman growth system, where germanium (Ge) doping gallium (Ga) was used as the model material. And we will compare the effects of ACRT and AVT in axial and radial direction. In next section, the experimental system and preparation are described briefly. Section 3 is devoted to results and discussion, and is followed by a short conclusion.

2. Experiment setup

The crystal was grown in quartz ampoules and coated with boron nitride in order to protect the ampoule and grown crystal; A sketch of the arrangement is shown in Fig. 1. The diameter of the seed and the growing crystal were 18 mm, the length of the seed was 40 mm and the length of the grown crystal was about 40-45 mm (shown in Fig. 2). Undoped germanium (1 1 1 orientated) served as the seed, the feed was pill-doped with gallium resulting in a dopant concentration (C_0). First, the germanium was rinsed with acetone followed by DI H_2O (18 MΩ). The ampoule was coated with boron nitride and baked under a proper procedure. Finally, the ampoule was sealed under an argon pressure of 0.08 torr (pressure at room temperature).

The growth experiment took place in an electrothermal furnace. The thermal gradient at the seed-feed interface is about 20 K/cm and monitored with K-type thermal couple. The ampoule was heated up with a constant rate of 10 ℃/min and kept at a constant temperature for 12 hours to guarantee a homogenous distribution of the dopant in the melt. For the growth process, the ampoule was pulled down at a constant velocity of 5.8 cm/hr from 0 to 29 mm at the beginning and 17.4 cm/hr from 29 mm to the end. After that, the furnace was cooled down slowly to the room temperature, for 14 hours. All the experiments are controlled under almost the same conditions (shown in Table 1).

After growth, the ingots were sliced along growing direction. They were polished and etched for 10 to 30 s by the solution of 1 part H_2O_2, 1 part CH_3COOH and 1 part HF volumetrically. In this treatment [13], the seed-feed interface was revealed. The axial and radial dopant concentration profiles were determined by resistitivity ρ obtained by four-point-probe measurements. The actual impurity concentration N (atoms/cm^3) was obtained using the following correlation [14] :

$$\rho = \mathbf{N}^{-\alpha}/\mathbf{B} \qquad (1)$$

where for p-type Ge (Ga-doped Ge), the values of α and B are indicated below in two different range of carrier concentration:

$B = 1.74\times10^{-11}$ and $\alpha = 0.707$
for $1\times10^{17} < N < 1\times10^{18}$
$B = 1.61\times10^{-10}$ and $\alpha = 0.653$
for $1\times10^{18} < N < 1\times10^{19}$

3. Results and discussion

3.1 Axial segregation

Fig. 3 and Fig. 4 show the axial dopant concentration profiles in the Ga-doped Ge crystal. In Fig. 3 and 4, the axial dopant concentration profile in comparison to Scheil [15], Tiller et al. [16], and experimental curves were illustrated. During directional solidification, solute transport takes place by diffusion and convection. Resultant axial dopant concentration profiles in the crystal have been calculated for the case of a purely diffusive (poor mixing) regime by Tiller et al. [16] and for the case of complete mixing (good mixing) of the melt by Scheil equation [15] with the following conditions:

a. seed-crystal interface is planar and perpendicular to the growth direction;
b. diffusion in the solid is negligible;
c. distribution coefficient k is constant ($k = 0.087$)

For a purely diffusive (poor mixing) regime, Tiller et al. [16] found Eq. (2) for the axial dopant concentration profile:

$$C_{s,D}(x) = C_0 [(1 - k) (1 - e^{-k v x / D_L}) + k] \quad (2)$$

where $C_{s,D}$ is concentration in the solid, C_0 is concentration in the melt at the beginning of the growth, v is the growth velocity in cm/min, x is solidified length and D_L is diffusion coefficient in the melt = 7.5×10^{-5} cm^2/s (see ref. [17]).

During growth with complete mixing in the melt the axial dopant concentration profile can be calculated with the Eq (3):

$$C_{s,c}(x) = k C_0 (1 - f)^{k-1} \quad (3)$$

where f = ratio of the solidified crystal = x/L, x = solidified length and L = the length of the crystal.

The resulting curve in Fig. 3 and 4 show the effects of AVT and ACRT in axial direction. In Fig. 3, the curves of 0Hz and 5Hz are almost no different in axial direction; it indicates that 5Hz AVT only causes the local mixing in the melt. In addition, after growing ~ 30 % long, the curve of 10Hz AVT closes to the good mixing curve. Because of the height of melt becomes short during growth process, the amplitude of 10Hz

AVT is strong enough to enhance the global mixing of the melt. The same condition is also discovered in 30 rpm ACRT experiment (shown in Fig. 4). Furthermore, the curve of 60 rpm ACRT is close to the good mixing curve at the beginning. It indicates that the external force of 60 rpm ACRT enhance the global mixing in the whole of melt.

3.2 Radial segregation

In Fig.5 and 6, the radial distributions are measured under low ampoule pulling rate and high ampoule pulling rate respectively. Without AVT or ACRT, it is clear that the concentration of center is much higher than the edge. In the experiment of low ampoule pulling rate, all the external forces can be an effective way to reduce the radial segregation. In the experiment of high ampoule pulling rate, only 10Hz AVT and 60 rpm ACRT can still maintain the symmetrical distribution. The concentration of the center will be a little enhanced in 5Hz AVT and 30 rpm ACRT experiments under high ampoule pulling rate.

4. Conclusions

In this paper, it is cleat that ACRT generates the global mixing, especially in 60 rpm ACRT experiment. On the other hand, angular vibration technique (AVT) can reverse the radial segregation easily and almost without enhancing global mixing, especially in 5Hz AVT experiment. Although both techniques can reduce the radial segregation, AVT is more effective for crystal growth control.

References

[1] H.J. Scheel, E.O. Schulz-Dubois, J. Crystal Growth 8 (1971) 304.

[2] P. Capper, J.J.G. Gosney, C.L. Jones, J. Crystal Growth 70 (1984) 356.

[3] W.G. Coates, P. Capper, J.J.G. Gosney, C.K. Ard., I.Kenworthy, A. Clark, J. Crystal Growth 94 (1989) 959.

[4] P. Capper, J.C. Brice, C.L. Jones, W.G. Coates, J.J.G. Gosney, C.K. Ard., I.Kenworthy, J. Crystal Growth 89 (1988) 171.

[5] P. Capper, J.J.G. Gosney, UK Patent 2098879A 1982.

[6] J.C. Brice Crystal Growth Process, Wiley, New York, 1986.

[7] A.Yeckel , J.J. Derby , J. Crystal Growth 209 (2000) 734.

[8] A.Yeckel , J.J. Derby , J. Crystal Growth 233 (2000) 599.

[9] W. C. Yu, Z. B. Chen, W. T. Hue, B. Roux, T. P. Lyubimova, C. W. Lan, J. Crystal Growth 271 (2004) 474.

[10] C. W. Lan, J. Crystal Growth 274 (2005) 379

[11] Y. C. Liu, B. Roux, C. W. Lan, J. Crystal Growth 304 (2007) 236

[12] Y. C. Liu, Z. B. Chen, W. T. Hue, B. Roux, T. P. Lyubimova, C. W. Lan, J. Heat Mass Transfer 50 (2007) 58.

[13] P.Dold, F.R. Szofran, K.W. Benz, J. Crystal Growth 234 (2002) 91.

[14] S.M.SZE and J.C.IRVIN, Solid-State Electronics 11 (1968) 599.
[15] E.Scheil, Z.Metallk. 34 (1942) 70.
[16] W.A. Tiller, K.A.Jackson, J.W. Rutter, B.Chalmers, Acta Metall.1 (1953) 428 .
[17] O. Madelung, M. Schulz and H. Weiss, Semiconductors Technology of Si, Ge and SiC, Landolt-Borbstein III/17 (Springer, Berlin, 1984) 12.

Table 1 Experimental parameters

		AVT		ACRT	
	0Hz	**5Hz**	**10Hz**	**30 rpm**	**60 rpm**
C_0 (atoms/cm^3)	5.01×10^{18}	1.24×10^{18}	1.07×10^{18}	1.96×10^{18}	1.95×10^{18}
L_s (cm)	4.2	4.2	4.2	4.2	4.1
G (K/cm)	≈20	≈20	≈19	≈20	≈21
***v* (cm/hr)**	5.8	5.8	5.8	5.8	5.8
v_g (cm/hr)	17.4	17.4	17.4	17.4	17.4

C_0 : dopant concentration, L_s : seed length, G : thermal gradient, *v* : pulling velocity, v_g quench velocity

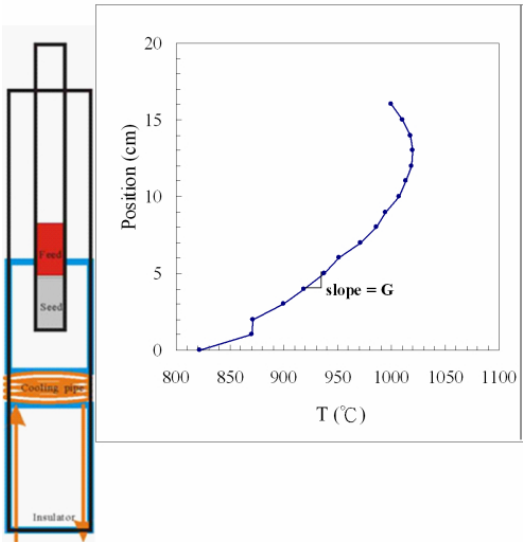

Fig. 1. A Sketch of experimental setup and its thermal profile.

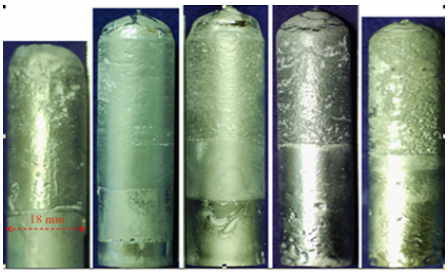

(a) (b) (c) (d) (e)

Fig. 2. The appearance of the grown crystals.
For (a) 0 Hz (b) 5 Hz (c) 10 Hz (d) 30 rpm ACRT (e) 60 rpm ACRT.

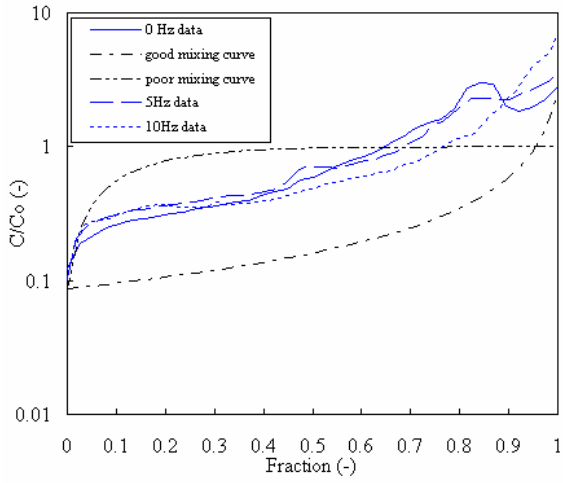

Fig. 3. Axial concentration profile (with and without AVT).

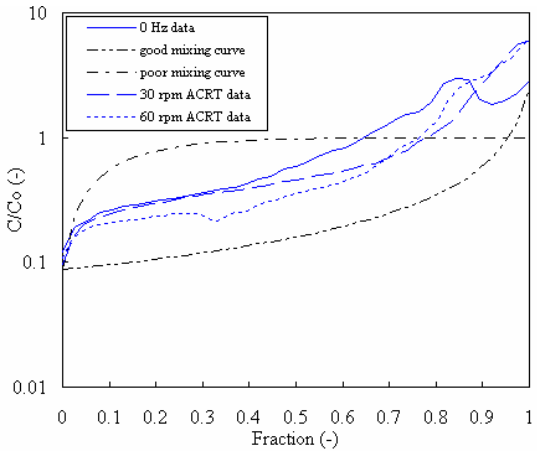

Fig. 4. Axial concentration profile (with and without ACRT).

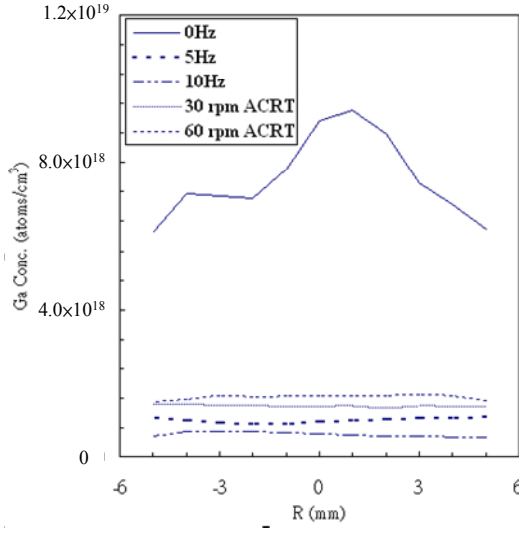

Fig. 5. Radial concentration profile (under low ampoule pulling rate).

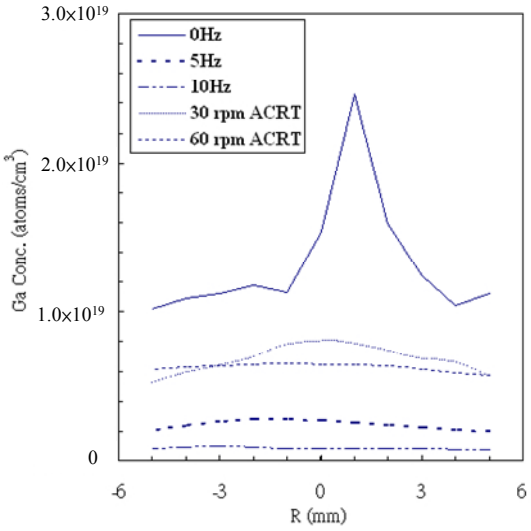

Fig. 6. Radial concentration profile (under high ampoule pulling rate).